

## Supporting Information

# Sensitive Field-effect Transistor Sensors with Atomically Thin Black Phosphorus Nanosheets

*Arnab Maity,<sup>a</sup> Xiaoyu Sui,<sup>a</sup> Haihui Pu,<sup>a</sup> Kai J. Bottum,<sup>a</sup> Bing Jin,<sup>a</sup> Jingbo Chang,<sup>a</sup> Guihua Zhou,*

*<sup>a</sup> Ganhua Lu<sup>a</sup> and Junhong Chen<sup>a,b,c,\*</sup>*

<sup>a</sup>Department of Mechanical Engineering, University of Wisconsin-Milwaukee, Milwaukee, WI 53211, USA. E-mail: [jhchen@uwm.edu](mailto:jhchen@uwm.edu)

<sup>b</sup>Current address: Pritzker School of Molecular Engineering, University of Chicago, Chicago, IL 60637, USA. E-mail: [junhongchen@uchicago.edu](mailto:junhongchen@uchicago.edu)

<sup>c</sup>Current address: Argonne National Laboratory, Argonne, IL 60439, USA. E-mail: [junhongchen@anl.gov](mailto:junhongchen@anl.gov)

## Supporting Information 1

**Table S1** The comparison of structural, electronic and sensing performance of various literature reports with present study.

Method	Thickness (nm) or Number of layer	Substrate and thickness	Top Protection Layer	On/Off Ratio	Contact Electrode deposition	Target ion, concentration and response%	Ref.
Scotch ME	16 nm (~22 layer)	SiO <sub>2</sub> 300 nm	--	~3.5	Cr-Au lithography	Mercury sensor (0.01-100 ppb) (1-10)	[1]
Scotch ME	40 nm (~57 layer)	SiO <sub>2</sub> 300 nm	Al <sub>2</sub> O <sub>3</sub>	~ 4.4	Gold Direct transfer	Human Ig-G sensor (10-500 ng/ml) (2-8)	[2]
Scotch ME	~12 nm (17 layer)	SiO <sub>2</sub> 300 nm	Ionophore	~2.2	Ti-Pd lithography	Lead Sensor (10-1000 ppb) (0.1-0.5)	[3]
Scotch ME	~80 nm (~114 layer)	SiO <sub>2</sub> 300 nm	Al <sub>2</sub> O <sub>3</sub>	~2.69	Gold Direct transfer	Arsenic (1-100 nM) (2-8)	[4]
Modified Scotch ME	(0.89-6.9) nm (~1-7 layer)	SiO <sub>2</sub> 300 nm	Al <sub>2</sub> O <sub>3</sub>	~100-502	Gold Selected area transfer	Lead sensor (1-400 ppb) (30±20 -900±200)	This Work

## References:

1. Li, P.; Zhang, D.; Jiang, C.; Zong, X.; Cao, Y. Ultra-sensitive suspended atomically thin-layered black phosphorus mercury sensors. *Biosens. Bioelectron.* **2017**, *98*, 68-75.

- Chen, Y.; Ren, R; Pu, H.; Chang, J.; Mao, S.; Chen, J. Field-effect transistor biosensors with two-dimensional black phosphorus nanosheets. *Biosens. Bioelectron.* **2017**, 89, 505-510.
- Li, P.; Zhang, D.; Liu, J.; Chang, H.; Sun, Y.E.; Yin, N. Air-Stable Black Phosphorus Devices for Ion Sensing. *ACS Appl. Mater. Interfaces.* **2015**, 7(44), 24396-24402.
- Zhou, G.; Pu,H.; Chang, J.; Sui, X.; Mao, S.; Chen, J. Real-time electronic sensor based on black phosphorus/Au NPs/DTT hybrid structure: Application in arsenic detection. *Sens Actuators B Chem.* **2018**, 257, 214-219.

## Supporting Information 2

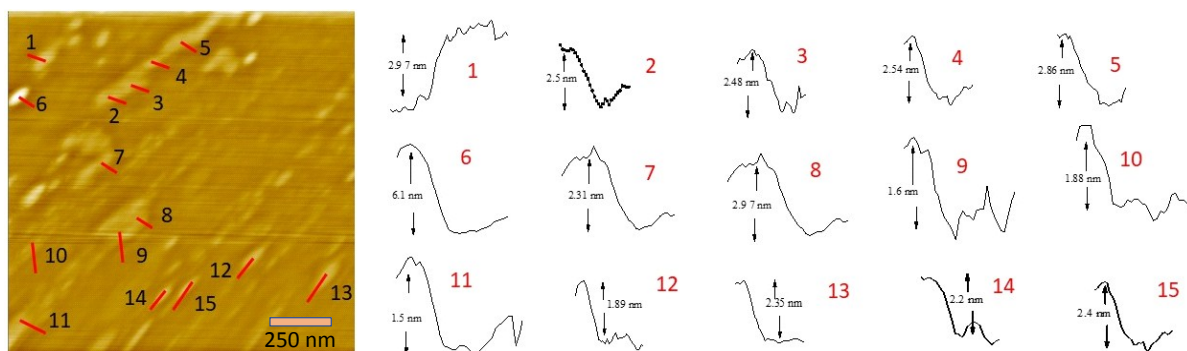


**Fig. S1** The thickness profile for AFM distribution of selected area devices.

### Supporting Information 3

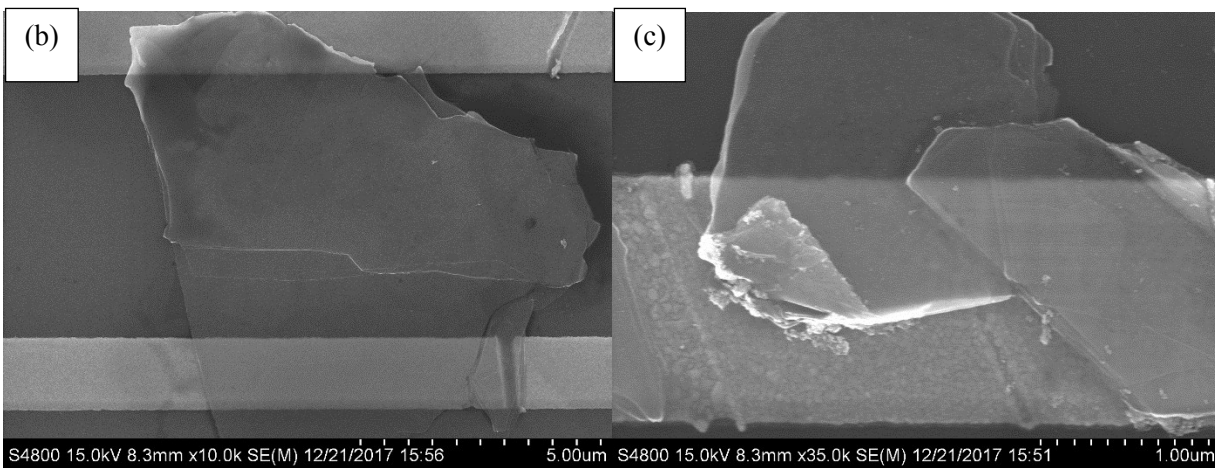


**Fig. S2 (a) and (b):** FESEM images of the BP nanosheet from random area sensors.

## Supporting Information 4

### Theoretical Modelling of the Thickness Dependence Response Pattern for Phosphorene FET Sensor

Assuming the device is operated in liner region, the current for gated FET in background DI water solution ( $I_{ds}$ ) and lead ion solution ( $I'_{ds}$ ) could be expressed as,

$$I_{ds} = \mu C_{ox} \frac{W}{L} [(V_{gs} - V_{th}) V_{ds} - \frac{V_{ds}^2}{2}] \quad (S1)$$

$$I'_{ds} = \mu C_{ox} \frac{W}{L} [(V'_{gs} - V'_{th}) V_{ds} - \frac{V_{ds}^2}{2}] \quad (S2)$$

where,  $V_{ds}$ ,  $V_{gs}$ , and  $V_{th}$  are the operating voltage across drain-source, top gate electrostatic potential ( $V_{gs}$ ) due to adsorption of lead ions on the cysteine modified surface, and threshold voltage, respectively.  $W$ ,  $L$ , and  $\mu$  are the width, length, and mobility of the channel that are invariant during gate voltage sweeping for specific phosphorene layer thickness. Now the response % (R) could be calculated using the relation,

The response % (R) could be calculated using the relation,

$$R = \frac{I_{ds} - I'_{ds}}{I_{ds}} = \frac{(V_{gs} - V'_{gs}) - (V_{th} - V'_{th})}{(V_{gs} - V_{th} - \frac{V_{ds}}{2})} \quad (S3)$$

Now, from the relation, we have  $qp = C_{ox}(V_{gs} - V_{th}) + qp_0$  and  $qp' = C_{ox}(V'_{gs} - V'_{th}) + qp_0$ , where,  $q$  is the charge,  $p$  and  $p'$  is the hole density before and after adding the lead ions. The sensitivity expression becomes,

$$R = \frac{p - p'}{\left(p - \frac{C_{ox} V_{ds}}{2q}\right)} = \frac{\Delta p}{(p - c)} \quad (S4)$$

Now, carrier density for hole from Boltzmann approximation,  $p = n_i \exp(E_i - E_F)/k_B T$

$$\begin{aligned} \Delta p &= [n_i \exp(E_i - E_F)/k_B T] - [n_i \exp(E_i - E_F - e\Delta\psi)/k_B T] \\ &= n_i \exp(E_i - E_F)/k_B T [1 - \exp(-e\Delta\psi/k_B T)] \\ &= n_s [1 - \exp(-e\Delta\psi/k_B T)] \end{aligned}$$

Here,  $\Delta\psi$  is the surface potential change due to the addition of lead ions. Since the second term

in the denominator of Eqn. S4 is constant ( $c = \frac{C_{ox} V_{ds}}{2q}$ ), the response % could be written as,

$$R = \frac{[1 - \exp(-e\Delta\psi/k_B T)]}{1 - \frac{c}{p}} \quad (S5)$$

The expression for charge density ( $p$ ) can be written as,

$$p = 2 \left( \frac{2\pi m_e m_h k_B T}{h^2} \right)^{3/2} \cdot \exp(-E_g/2k_B T) \cdot \exp(E_i - E_F)/k_B T \quad (S6)$$

Combining Eqn. S5 and S6, the sensitivity expression can be approximated as,

$$R \sim \exp\left(\frac{E_g}{2k_B T}\right) \cdot \exp(|E_i - E_F|)/k_B T \quad (S7)$$

It is to be noted that this model for sensitivity variation upon BP layer thickness is based on a single gate voltage difference value equivalent to a single concentration of lead ions. The idea was to simulate the effect of BP layer thicknesses on the sensitivity (relative current change in the presence of lead ions) for a certain gate oxide thickness. The top and bottom gates could be equivalently transferred using the relation between threshold voltage, dielectric constant,

geometry, and capacitive coupling factor. The capacitive coupling amplifies a change in top-gate threshold voltage ( $\Delta V_{T,top}$ ) which consequently results in an amplified shift in bottom-gate threshold voltage ( $\Delta V_{T,back}$ ) that depends upon the capacitance of the liquid-exposed top-gate dielectric ( $C_{top}$ ), the back-gate dielectric ( $C_{back}$ ) and a factor ( $\alpha_{SN}$ ) with a value between 0 and 1 depending on the extent of coupling due to the choice of biasing conditions:

$$\Delta V_{T,back} = \Delta V_{T,top} \frac{C_{top}}{C_{back}} \alpha_{SN} \quad (S8)$$

For known values of thickness, area and dielectric constant of the top and bottom gate oxides, the relationship could be interchangeable.

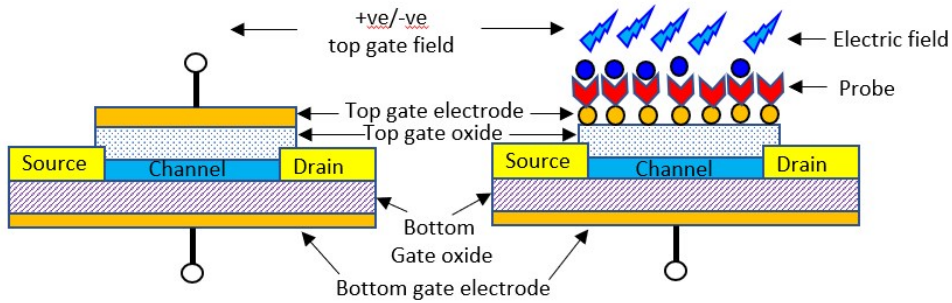


**Fig.1:** Comparison of the schematic model of MOSFET and dielectric gated FET sensor

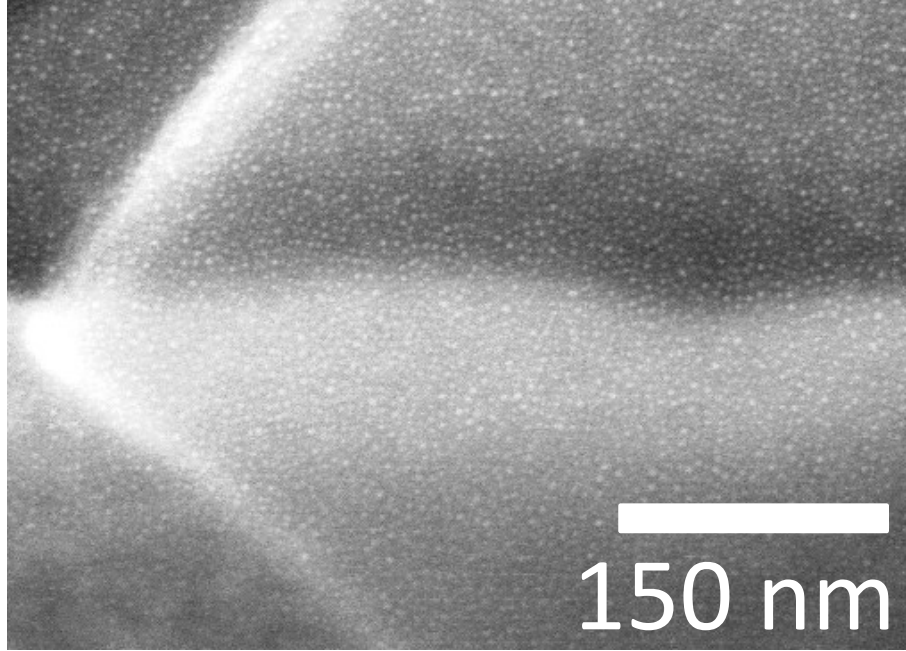


**Fig.2:** High magnification image of sputtered granular gold nanoparticles on ALD coated FET sensor device.

It is also to be noted that surface potential change due to the top gate by lead ion adsorption is related with the probe density which is dependent on the density of gold nanoparticles on the top gate dielectric. From the FSEM image, it is clear that sputtering-deposited gold nanoparticles are highly dense, and thus a uniform surface potential is expected throughout the active area of the sensor. Using the Grahame equation, the surface potential ( $V_d$ ) could be calculated based on the Gouy-Chapman theory.

$$V_D = \frac{2k_B T}{ze} \sinh^{-1} \left( \frac{\sigma_D T}{\sqrt{8 k_B T \epsilon \epsilon_0 C^\infty}} \right) \quad (S9)$$

Where,  $K_b$ ,  $T$ ,  $Z$ ,  $e$ ,  $\epsilon$ ,  $\epsilon_0$ ,  $\sigma_D$ ,  $C^\infty$  are the Boltzmann constant, temperature in Kelvin, charge of the ion, electronic/protonic charge, dielectric constant of medium and air, charge density on the sensor surface at liquid medium, lead ion concertation. It is also to be noted that the top gate oxide of the sensor is considered as an ideal dielectric; i.e., no leakage current influence is

present in the present model. The influence of the leakage current could create a competitive effect in the measured current. Thus, a thicker top gate dielectric with a high dielectric constant is preferred for reducing the leakage current from the solution to obtain an ideal response transient.

## Supporting Information 5

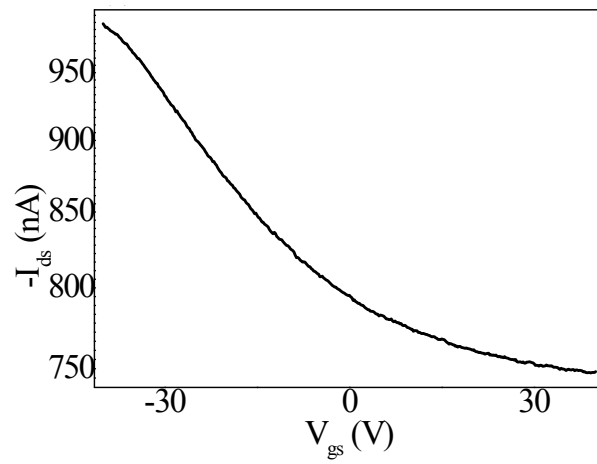


**Fig. S3.** Plot of  $V_{gs}$ - $I_{ds}$  characteristics curve of random PFET device for  $V_{ds} \sim -0.01$  V and  $V_{gs} \sim -40$  V to 40 V.

## Supporting Information 6

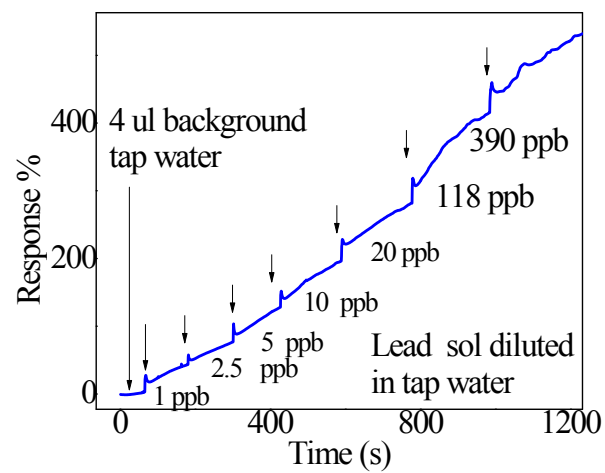


**Fig. S4.** The tap water sensing performance spiked with various lead ion concentrations for selected area based PFET sensors.

## Supporting Information 7

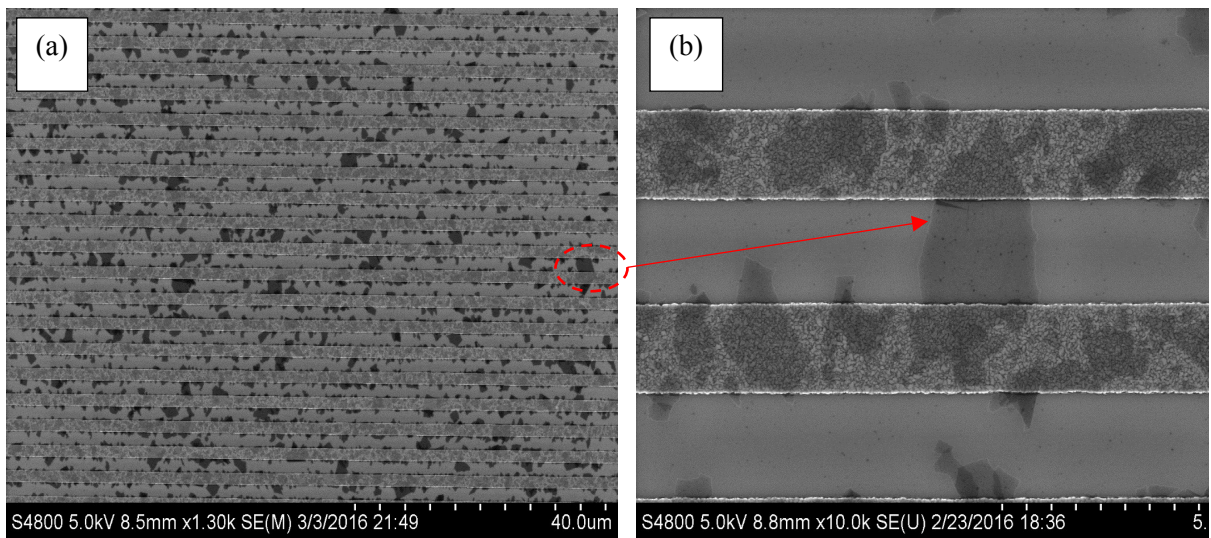


**Fig. S5.** FESEM images of rGO based sensors at (a) low and (b) higher magnifications.

## Supporting Information 8

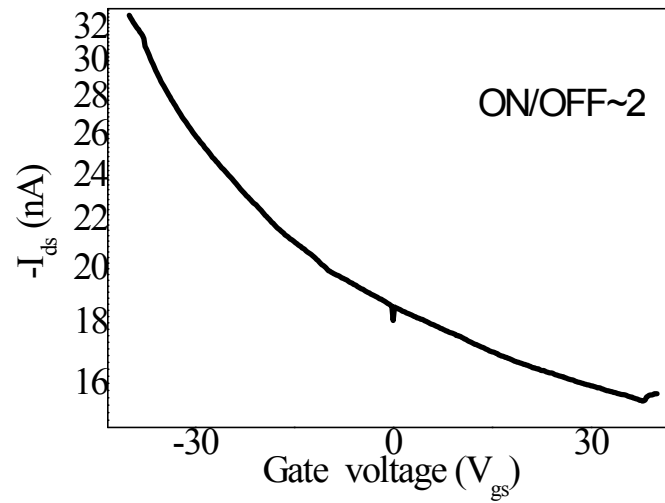


**Fig. S6.** Plot of  $V_{gs}$ - $I_{ds}$  characteristics curve of rGO FET sensor for  $V_{ds} \sim -0.01$  V and  $V_{gs} \sim -40$  V to 40 V.

## Supporting Information 9

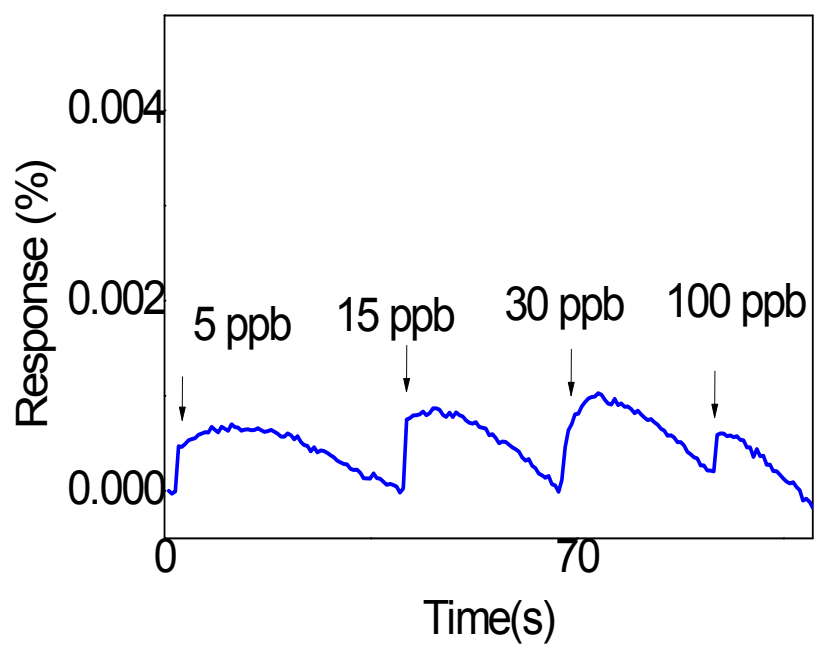


**Fig. S7.** Plot of sensing test for BP/Al<sub>2</sub>O<sub>3</sub>/Au (without cysteine probe functionalization).

## Supporting Information 10

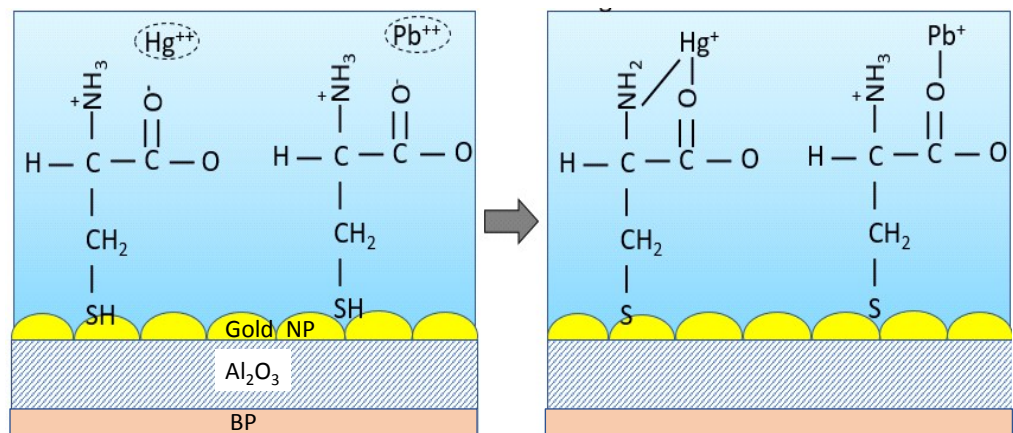


**Fig. S8.** Schematic representation of cysteine-heavy metal interaction.